International Journal of Nanoelectronics and Materials
Volume 11, No. 2, Apr 2018 [179-194]

Synthesis and Characterization of Zinc Oxide Nanoparticles using Green and Chemical Synthesis Techniques for phenol decontamination

H. Shokry Hassan[1*], M. F. Elkady[2,3**], E.M. El-Sayed [3] A. M. Hamed[4], A. M. Hussein[4] and Islam M. Mahmoud[4]

[1]*Electronic Materials Researches Department, Advanced Technology and New Materials Research Institute, City of Scientific Research and Technological Applications, New Borg El-Arab, 21934, Alexandria, Egypt.*
[2]*Chemical and Petrochemical Engineering Department, Egypt-Japan University of Science and Technology, New Borg El-Arab, Alexandria, Egypt.*
[3]*Fabrication Technology Researches Department, Advanced Technology and New Materials Research Institute, City of Scientific Research and Technological Applications, New Borg El-Arab, 21934, Alexandria, Egypt.*
[4]*Chemistry Department, Faculty of Science Al-Azhar University, Al-Azhar uni Street, 71524 Assiut, Egypt.*

Received 27 September 2017; Revised 24 October 2017; Accepted 6 December 2017

ABSTRACT

Zinc oxide nanoparticles (ZnO-NPs) were successfully synthesized using both biological and chemical techniques. This study is mainly focused on the green synthesis (biological) method of ZnO-NPs using different plant leaf extracts from leaves of guava, olive, fig, and lemon. The plant leaf extracts (polyphenols) act as reductants and zinc nitrate hexahydrate ($Zn(NO_3)_2.6H_2O$) acts as a precursor. Chemical synthesis method of ZnO-NPs was carried out using prepared sodium hydroxide and zinc nitrate. The produced ZnO-NPs were characterized using X- ray diffraction (XRD), scanning electron microscope (SEM), transmission electron microscopy (TEM), fourier transform infrared (FTIR), Thermal gravimetric analysis (TGA), and particle size analysis (PSA). The average crystallite size of green-synthesized zinc oxide nanopowders range from 7.1 to 28 nm, while the average crystallite size of chemical-synthesized zinc oxide powders range from 19.6 to 148 nm according to the XRD calculations and TEM observations. Both ZnO nanopowders showed high thermal stability up to 600 ^oC. The green-synthetized ZnO-NPs were evaluated for phenol decontamination in polluted wastewater. The maximum recorded phenol removal was 99.7% within 250 minutes using 0.1g ZnO-NPs, making ZnO-NPs a promising adsorbent material for phenol decontamination in polluted wastewater.

Keywords: Zinc Oxide Nanoparticles (ZnO-NPs), Green Synthesis, Biological and Chemical Synthesis, Plant Leaf Extract, Phenol Removal.

1. INTRODUCTION

The growth and development of mankind have always been closely associated with the progress of materials technology. In the last decades, the field of nanotechnology and associated researches were continuously in rapid growth due to the experience and capitalization of accumulated knowledge [1]. A large variety of nanomaterials has attracted more consideration because of their desirable properties and the possibility to be used in innovative technology applications [2,3]. A nanoparticle can be defined as a small object that

*Corresponding Author : *marwa.f.elkady@gmail.com*

acts as a whole unit in terms of its transport and properties. The engineering and science technology of nano-systems are considered the most demanding and rapid-growing areas of nanotechnology. Physical and chemical processes are convenient for nanoparticle synthesis, but the use of toxic compounds restricts their application [4].

Zinc oxide has been an essential material for industries for centuries and is presently the subject of a significant new interest. ZnO is a white powder that is insoluble in water that is already widely used in our society as an additive in numerous materials and products. Indeed it is a key element in many industrial manufacturing processes but most zinc oxides are prepared synthetically [5]. It is well known that the sizes, phases, and morphologies of the nanomaterials have a large impact on their properties and technological applications. Therefore, many researchers have focused on the control of the morphological structures of nanomaterials in their researches [6].

Biosynthesis of nanoparticles has gained significant importance in recent years and has become one of the most preferred syntheses [7-9]. In the biosynthesis method of ZnO NPs, plant leaf extract is used for a controlled synthesis of zinc oxide nanoparticles, using the aqueous extract of different plant leaves as reductant to develop an environmentally friendly process through biomimetic approaches rather than the traditional methods that use various routes for the synthesis of ZnO NPs.

These techniques in general can be divided into three: chemical, physical, and biological method. Chemical synthesis can be further divided into liquid and gas phase synthesis. Liquid phase synthesis includes the following 10 methods; precipitation, coprecipitation [10], colloidal, sol-gel processing [11], water–oil microemulsions [12], hydrothermal synthesis [13], solvothermal, sonochemical [14], polyol [15], and vapor phase method [16]. Fabrications such as pyrolysis, inert gas condensation methods, and laser ablation are classified as physical methods [17]. However, these mentioned techniques are extremely expensive and have many disadvantages due to the difficulty of scaling-up the process of synthesis, separation, and purification of nanoparticles from surfactants, co-surfactants, organic solvents, and toxic materials, which involve use of toxic, hazardous chemicals like borohydride, hydrazine hydrate, citrate, and hydrazine hydrochloride as reductants.

Phenols are considered one of the top 45 most important risky substances that are required to be treated before its release into the environment, as referred from the Agency for Toxic Substances & Disease Registry, USA classification. Indeed, even at a low concentration, phenols have decimating effects on life forms such as sour mouth, diarrhea, impaired vision, and excretion of dark urine [18].

Recently, the growth of awareness towards green chemistry and other biological processes have led to the improvement of rapid, cost-effective, and eco-friendly biosynthesis of zinc oxide Nano powder using the plant leaf extract approach for the synthesis of nanoparticles [19]. This study compares the physico-chemical properties of ZnO nano powder materials produced from chemical and biological routes.

2. MATERIAL AND METHODS

2.1 Materials

Pure, high grade Zn $(NO_3)_2.6H_2O$ and NaOH were supplied by Sigma-Aldrich chemicals. Fresh plant leaves of guava, olive, fig, and lemon were collected early in the morning during the month of May 2016 from Sohag – Egypt.

2.2. Extraction of the Antioxidants (Poly Phenols) from Plant Leaves

Plant leaf extracts were collected from fresh plant leaves of olive, guava, fig, and lemon. These leaves were collected, washed with water and distilled water for dust removal, and then dried overnight in an oven at 70°C. Then, the dry leaves were grinded into fine powder. The extract that would be used for the reduction of zinc ions (Zn^{2+}) to (ZnO) nanoparticles was prepared by placing 12.5g of dried leaves in a 250ml beaker filled with 200ml of water. The mixture was then boiled for 2 hours at 60-80˚C using a stirrer heater until the color of the aqueous solution changed from watery to light yellow. The extract was cooled to room temperature and filtered using filter paper. The extracted filtrate was stored in a refrigerator and used as a reducing agent [20].

2.3. Synthesis of ZnO Nanoparticles

ZnO NPs were prepared in two ways; chemically and through green synthesis using sodium hydroxide and the plant leaf extracts collected from fresh and dry plant leaves of olive, guava, fig, and lemon.

2.3.1. Biosynthesis of ZnO nanoparticles

In this method, liquid extract of antioxidants (poly phenols) from the plant leaves was used for zinc salt reduction. 70ml of $Zn(NO_3)_2.6H_2O$ with a concentration of 0.2 M was reduced by 30ml of (olive, guava, fig, lemon) leaves extracts (stored in refrigerator). These extracts were added under constant stirring, dropwise, and then boiled to 60˚C using a stirrer-heater for 1 hour. The produced powder materials were dried at 100°C overnight. During the drying process, complete conversion of zinc hydroxide into zinc oxide took place until the oxide turned into a dark yellow-colored paste. This paste was collected in a ceramic crucible and calcinated at 500˚C for 2 hours. A sunny yellow powder was produced after the calcination process. The material was grinded after calcination to produce fine powder. The schematic diagram of the ZnO biosynthesis method is shown in Figure 1 [20,21].

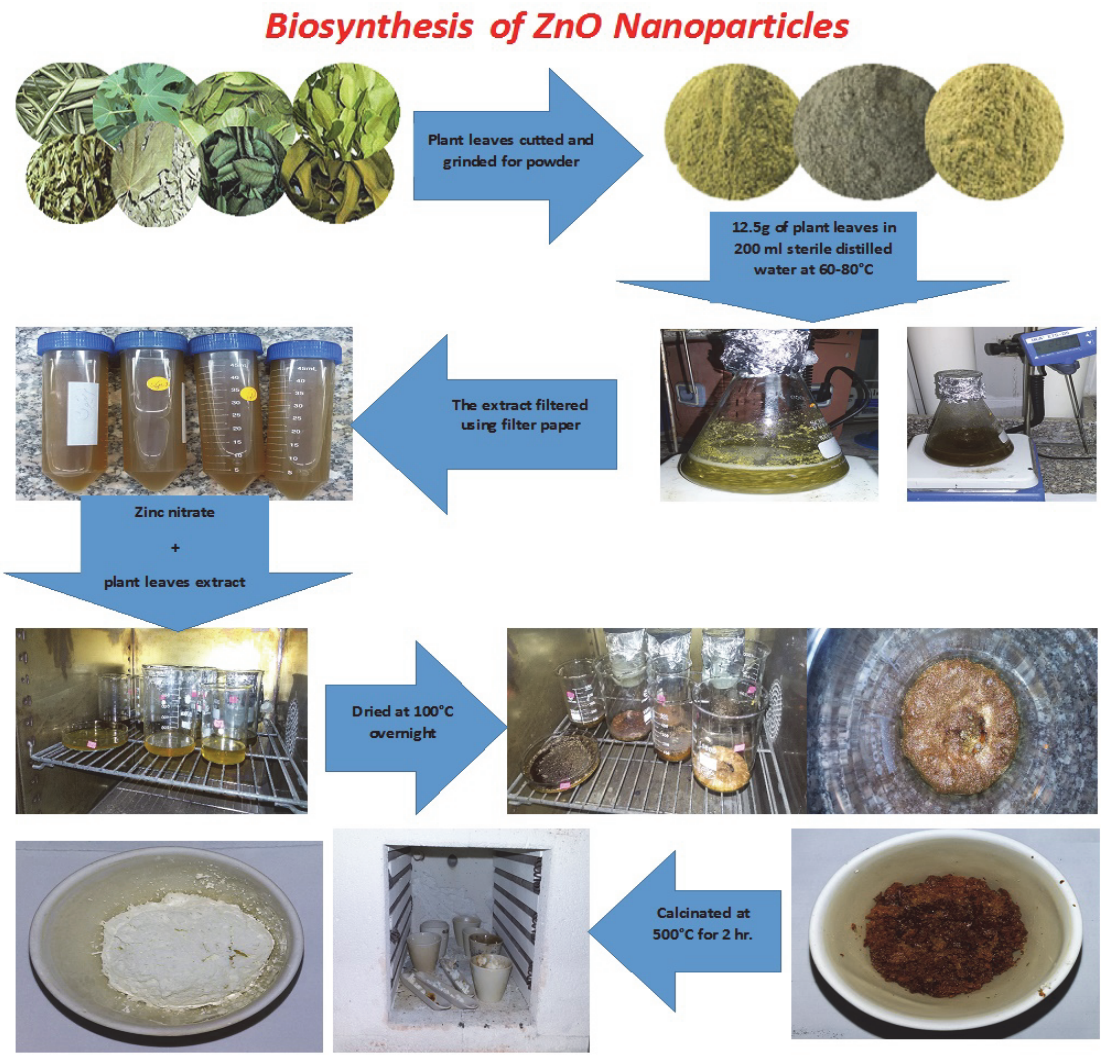

Figure 1. Biosynthesis of ZnO nanoparticles schematic diagram.

2.3.2. Chemical Synthesis of Zinc Oxide Nanoparticles

The facile sol-gel technique was used for zinc salt reduction. The solution of $Zn(NO_3)_2.6H_2O$ at a concentration of 0.2 M was reduced using a 9.8ml of 2 M sodium hydroxide. The reducing agent was added dropwise under constant stirring until the solution's pH reach 12. After the complete addition of NaOH, the reaction continued for 2 hour. The solution was kept overnight and the produced solid materials were separated using centrifugal force. The separated powder materials were washed using distilled water. Finally, the materials were dried at 100°C. During the drying process, the conversion of zinc hydroxide into ZnO took place [22].

2.4. Characterization of the Prepared Zinc Oxide Nanoparticles

X-ray diffraction patterns of the nanopowders were obtained using a (Schimadzu 7000) diffractometer, operating with Cu Kα radiation (λ = 0.15406nm). The patterns were generated at 30kV and 30mA with a scan rate of 2° min^{-1} for 2θ values between 20 and 80 degrees. Scanning electron microscope (SEM) analyses (JEOL JSM 6360LA, Japan) were performed to determine the shape and morphology of ZnO nanoparticles. The morphology and size of the prepared ZnO materials were detected using TEM (JEOL JEM 1230, Japan). FTIR spectrums of the prepared ZnO materials were established using (Shimadzu FTIR-8400 S, Japan) at a wavelength range of 400 – 4000 cm^{-1}. The thermal stability of the prepared ZnO was evaluated

through thermo gravimetric analysis (TGA) using a Thermo Gravimetric Analyzer (ShimadzuTGA–50H, Japan). The particle size of the ZnO material and its distribution were determined using a particle size analyzer (PSA) (LA-960 combines).

2.5. Assessment of the Green Synthetized ZnO-Nps for Phenol Sorption

The affinity of green-synthetized ZnO-NPs toward phenol sorption was verified using synthetic polluted water in a batch manner. The phenol sorption profiles of 0.1g of green-synthetized ZnO-NPs were determined against contact time (0-250 min). The percentage of the removal of phenol using tested ZnO-NPs was estimated from equation (1)

$$\% \text{ Removal} = ((C_o - C) / C_o) * 100 \quad (1)$$

where C_o is the initial phenol concentration in the solution (mg/l), and C is the final phenol concentration after treatment process (mg/l).

3. RESULTS AND DISCUSSION

The end product of the successfully synthesized zinc oxide nanoparticles using the green-synthesis method is light yellow-colored powder precipitate, while the product of the chemical synthesis method is white precipitate.

Bio-reduction of the zinc ions (Zn^{2+}) to ZnO during exposure to the plant leaf extracts was followed by a color change from pale yellow to yellowish brown after the drying process. From the chemical synthesis method, zinc salt was reacted with sodium hydroxide to produce zinc hydroxide and sodium nitrate. This hydroxide decomposes upon heating to zinc oxide. Both green and chemical preparation techniques of ZnO nanomaterials depend on a spontaneous reduction of zinc salt shown as Eq. (2) and (3).

$$Zn(NO_3)_2 + 2NaOH \rightarrow Zn(OH)_2 + 2NaNO_3 \quad (2)$$
$$Zn(OH)_2 \rightarrow ZnO + H_2O \quad (3)$$

During the decomposition of $Zn(OH)_2$ into ZnO nanoparticles, the yield obtained was 1.6 g which means about 60% of the precursor used was converted into pure ZnO nanoparticles using the green synthesis method. However, this production yield of ZnO nanoparticles increased to 87% when the chemical preparation technique was used.

3.1 XRD Analysis

XRD was used to characterize the different methods used to prepare the ZnO nanopowders. Figure 2 shows the XRD pattern for the ZnO nanopowder synthesized by both chemical and green techniques using extracts from fresh and dry plant leaves of olive, guava, fig, and lemon. X-ray diffraction of the Zinc oxide NPs synthesized using the chemical method with zinc nitrate and sodium hydroxide as materials is studies based on Figure 2 (A). It is indicated from this figure that distinctive peaks appear at (100), (002), (101), (102), (110), (103), (200), (112) and (201). The results confirm that the prepared ZnO nanoparticles are of wurtzite hexagonal structure and show a high degree of crystallinity.

The X-Ray diffraction pattern of the sample synthesized from aqueous plant leaf extract using the green synthesis method is illustrated in Figure 2 (B_1, B_2, C_1, C_2, C_3, C_4). It indicates that the distinctive peaks that appear at (100), (002), (101), (102), (110), (103), (200), (112), and (201) are in good agreement with wurtzite ZnO (JCPDS CARD NO: 36- 1451) [23]. The X-ray pattern clearly demonstrates that all diffraction peaks of the prepared ZnO NPs have high

purity and degree of crystallinity structure. The X-ray diffraction peaks clearly demonstrate that fresh and dry plant leaf extracts result in green-synthesized ZnO NPs with same diffraction peaks without any changes. The sharp and narrow diffraction peaks indicate that the product is well crystalline in nature. The mean crystalline size (D) of the particles was determined from the XRD line broadening measurement using Scherrer equation equation 4.

$$D=0.89\lambda / (\beta Cos\theta) \quad (4)$$

Where D is the mean size of crystallites (nm), K is the Scherrer constant crystallite shape factor with a good approximated value of 0.9, λ is the 0.1541nm wavelength of the x-ray source (Cu Kα) used in XRD, B is the full width at half the maximum of the diffraction peak (FWHM) in radians of the X-ray diffraction peak, and θ is the Bragg (diffraction) angle. The XRD peaks from the green synthesis method are not as sharp as those from the chemical synthesis method. This shows a slight decrease in crystallinity, which suggests the formation of particles of smaller size. The calculated average crystalline size of zinc oxide nanoparticles prepared using the chemical synthesis method is 19.6nm, and is reduced to 8.5, 9.49, 7.10, 10.34, 9.3, and 13.76nm when the chemical synthesis was replaced by the green synthesis using extracts from different fresh and dry plant leaf extracts of olive and guava, and dry plant leaf extracts of fig and lemon respectively. It can be clearly seen that the broadening of peaks from the green synthesis method using extracts of olive and guava and dry plant leaf extract of fig and lemon is greater compared to those from the chemical synthesis method, indicating that the green-synthesized particles have smaller particle sizes [24, 25].

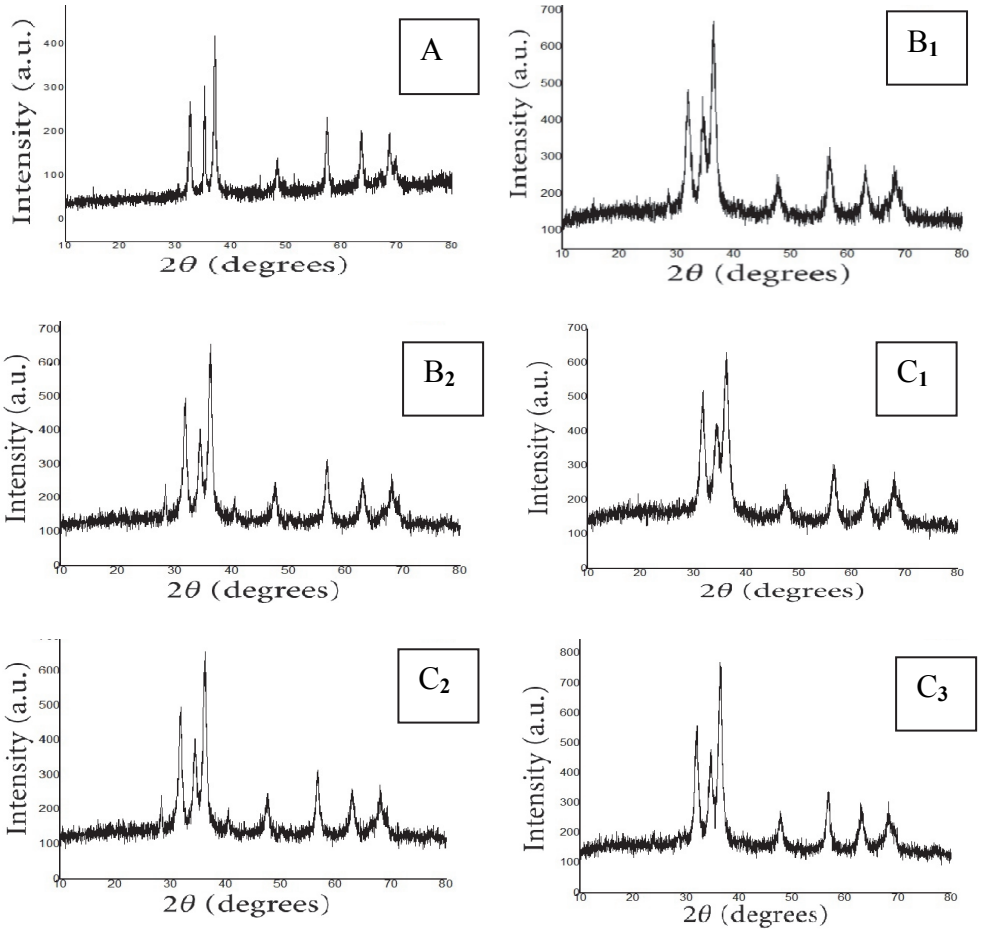

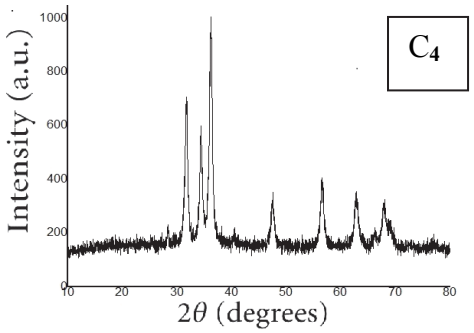

Figure 2. XRD spectrums of synthesized pure nano zinc oxide using both chemical and green synthesis methods: (A) chemical, (B_1) olive fresh, (B_2) guava fresh, (C_1) olive dry, (C_2) guava dry, (C_3) fig dry and (C_4) lemon dry.

3.2 SEM Analysis

The scanning electron microscope (SEM) analysis was performed to determine the shape and morphology of pure ZnO nanoparticles under various magnifications and the results are depicted in Figure 3. The SEM results of the studied ZnO nanoparticles synthesized using both chemical and green synthesis method using the extracts from fresh and dry plant leaves of olive, guava, fig, and lemon reveal the formation of stable ZnO nanoparticles. The SEM images show spherical, spongy, and irregular shapes of ZnO nanoparticles in addition to individual zinc particles as well as a number of agglomerates. The SEM image (Figure 3) shows that the particle size of green-synthesized zinc oxide nanoparticles (Figure 4 from B_1-C_4) is comparatively smaller than the chemical-synthesized nanoparticles (Figure. 3 A) and the particle size of fresh green-synthesized, spherical shaped zinc oxide nanoparticles (Figure 3 B_1, B_2) is comparatively smaller than the dry green-synthesized irregular and spongy zinc oxide nanoparticles (Figure 3 C_1, C_2, C_3, C_4). These results are in good agreement with the XRD results [21].

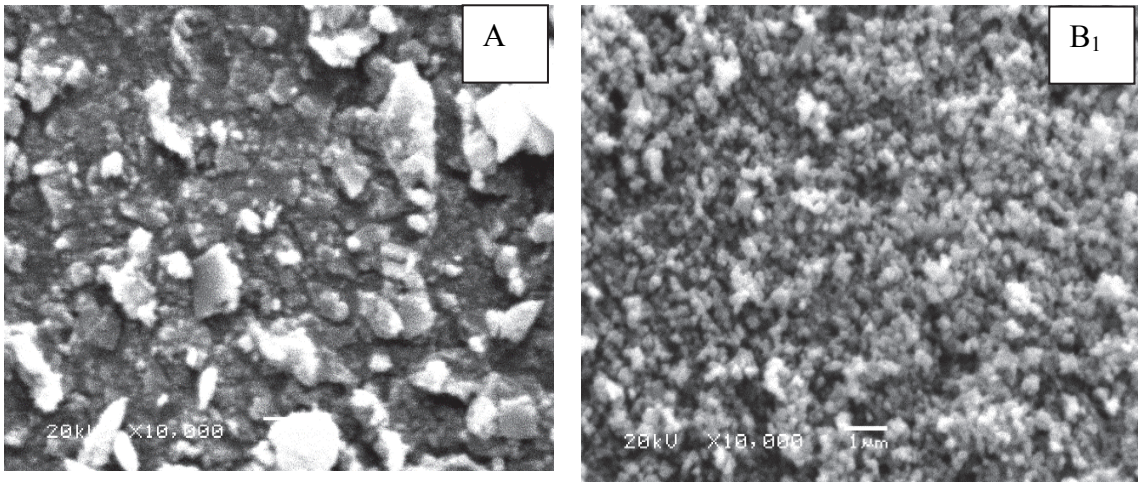

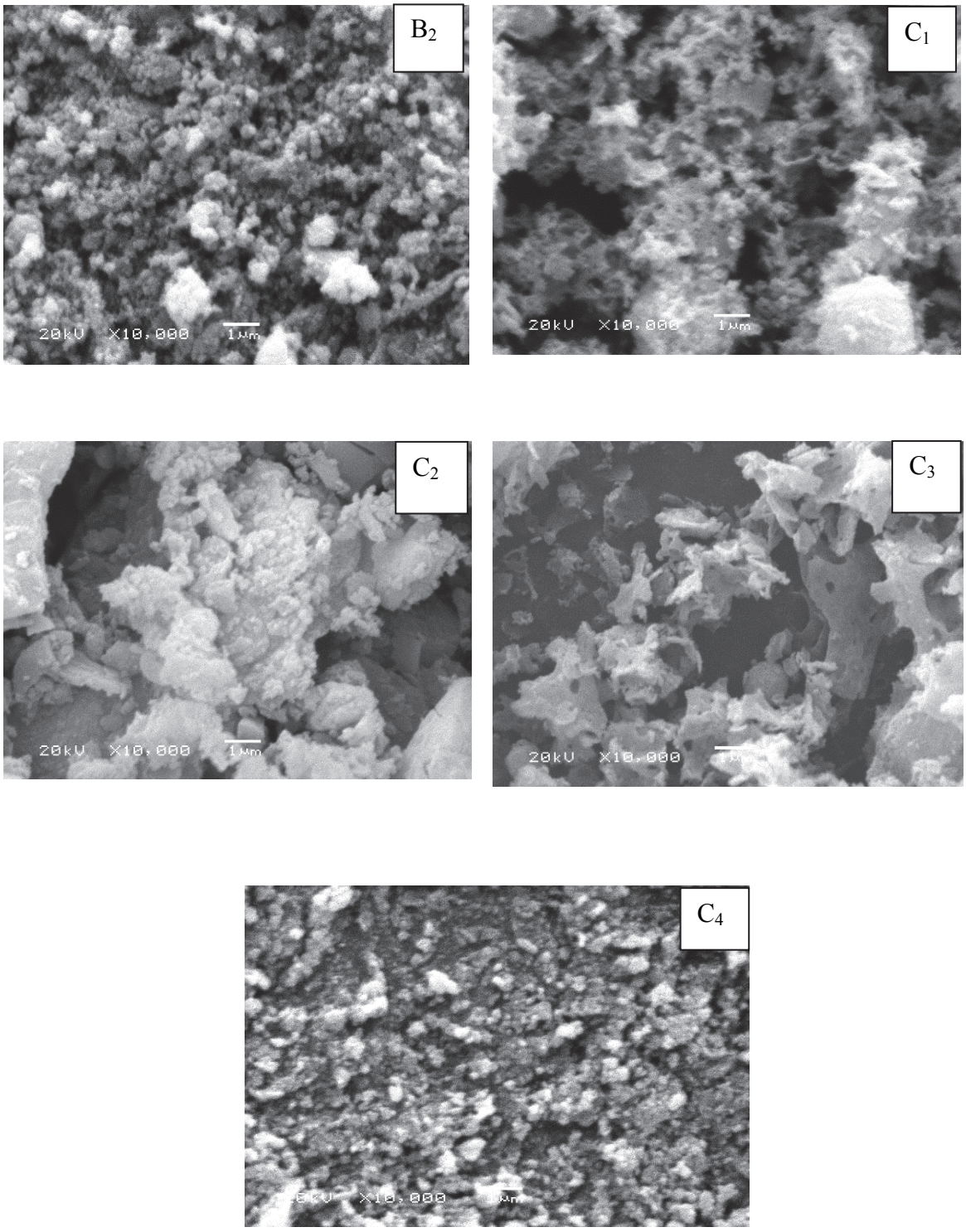

Figure 3. SEM Analysis of synthesized pure nano zinc oxide by both chemical and green synthesis methods: (A) chemical, (B_1) olive fresh, (B_2) guava fresh, (C_1) olive dry, (C_2) guava dry, (C_3) fig dry and (C_4) lemon dry.

3.3 Transmission Electron Microscopy (TEM)

Figure 4 shows the TEM images of the ZnO nanoparticles synthesized with a zinc nitrate precursor through both chemical (A) and green synthesis, using different fresh and dry plant leaf extracts of olive, guava, fig, and lemon ($B_{1.1}$,$B_{1.2}$), B_2, C_1, C_2, C_3 and C_4). It can be

observed that the particles synthesized using both methods have almost-spherical shapes with small agglomeration, except when fresh olive plant leave extracts were used for the green synthesis method where the resulting particles have nano rod shapes with an average size between 12-48nm, as shown in Figure 4 ($B_{1.1}$). The average particle size of ZnO from the chemical synthesis method was found to be from 44 to 145nm. When sodium hydroxide was replaced by fresh and dry plant leaf extracts of olive, guava, fig, and lemon and the same procedure was conducted, the average size of the particles reduces to 7.32 to 28nm. These results are in good agreement with the XRD results. A well-dispersed rod-like structure with an average diameter of 8.9-21nm produced using fresh olive plant leaf extract was observed, which is also in relative agreement with the XRD results. It is clear from the TEM study that the average diameters of the ZnO NPs are almost the same even if the extracts were used from different Fresh and dry plant leaves of olive, guava, fig, and lemon [26].

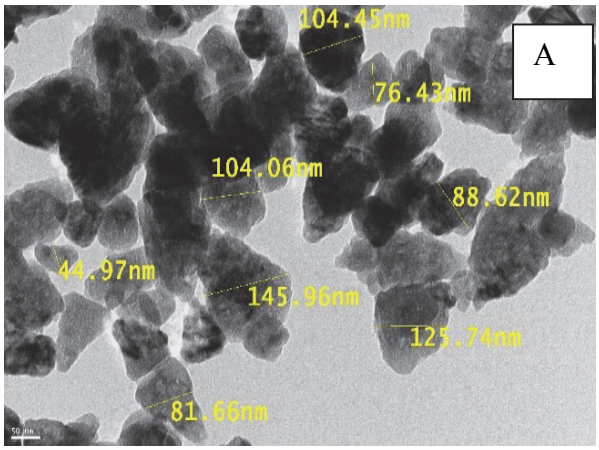

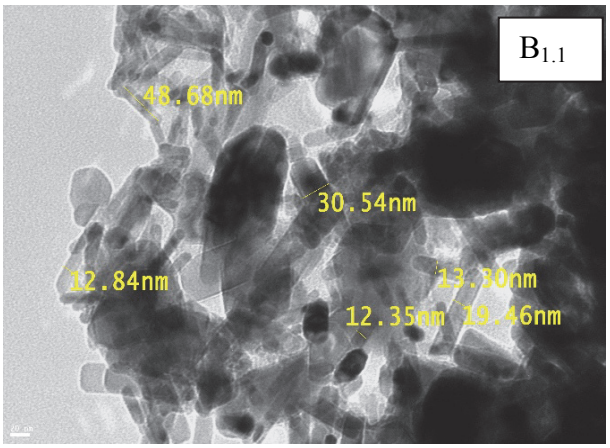

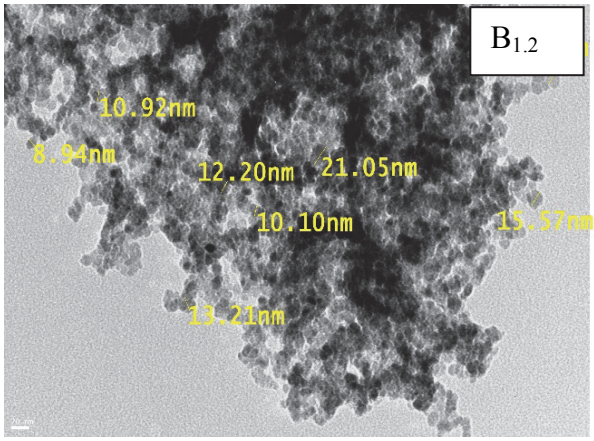

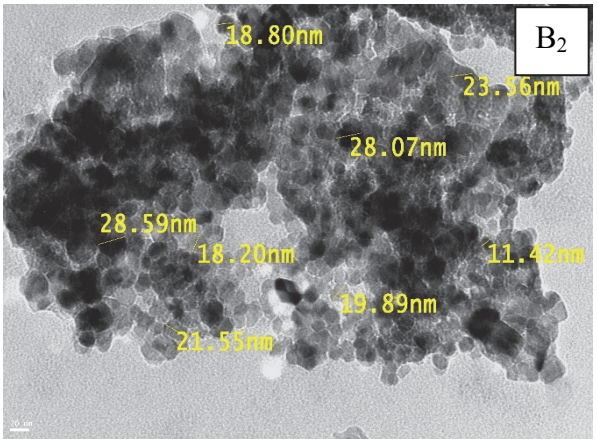

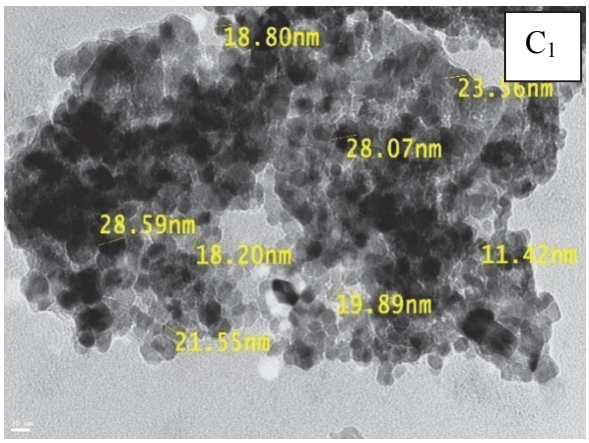

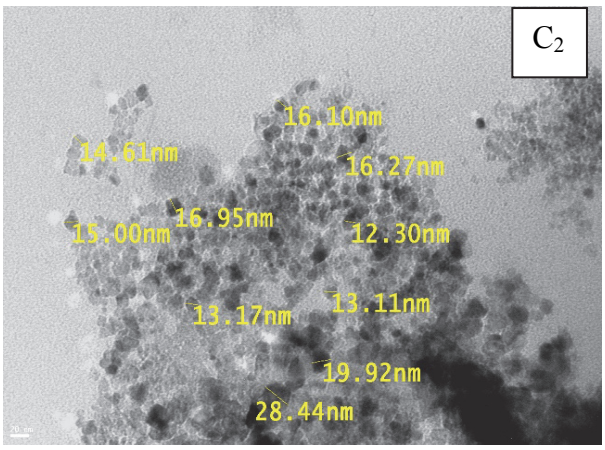

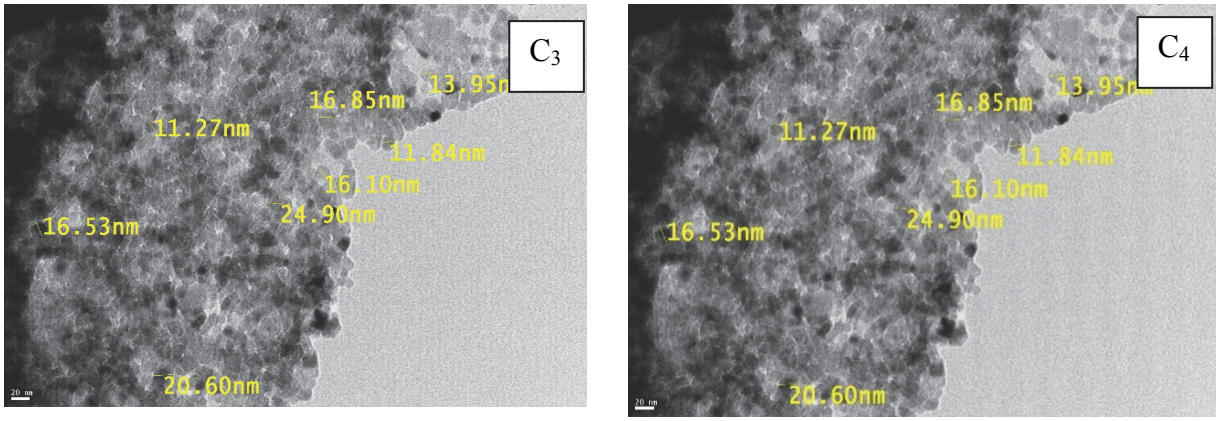

Figure 4. TEM images of the ZnO nanoparticles synthesized using both chemical and green synthesis methods: (A) chemical, ($B_{1.1}$, $B_{1.2}$) olive fresh, (B_2) guava fresh, (C_1) olive dry, (C_2) guava dry, (C_3) fig dry and (C_4) lemon dry.

3.4 FTIR Spectroscopy

Figure 5 (A, B_1) is recorded in the wavelength range of 400cm^{-1} to 4000cm^{-1} and shows the FTIR spectra of ZnO nanoparticles synthesized by chemical (Figure 5 (A)) and green (Figure 5 (B_1)) methods using plant leaf extracts. Generally, ZnO nanoparticles have characteristic absorption bands in region below 1000 cm^{-1} due to inter-atomic vibrations. The broad peak resulted from the chemical synthesis method is observed at 3439.19 and 1103.32cm^{-1} while from the green synthesis method the broad peak is observed at 3398.89 and 1035.81 cm^{-1}, which correspond to O-H stretching band or may be due to water adsorption on the metal surface. The peaks at 1639.55, 1635.69cm^{-1}, 1456.30cm^{-1} and all bands at 449.43-557.45cm^{-1} are attributed to ZnO nanoparticles that correspond to Zn-O's stretching and deformation vibration respectively. The broad peak at 1456.30cm^{-1} is due to the effect of polyphenols and natural pigments from the plant leaf extracts. The broad peak at 3398.69 and 3439.19cm^{-1} are due to metal-oxygen (metal oxides) frequencies observed for the respective ZnO nanoparticles [7].

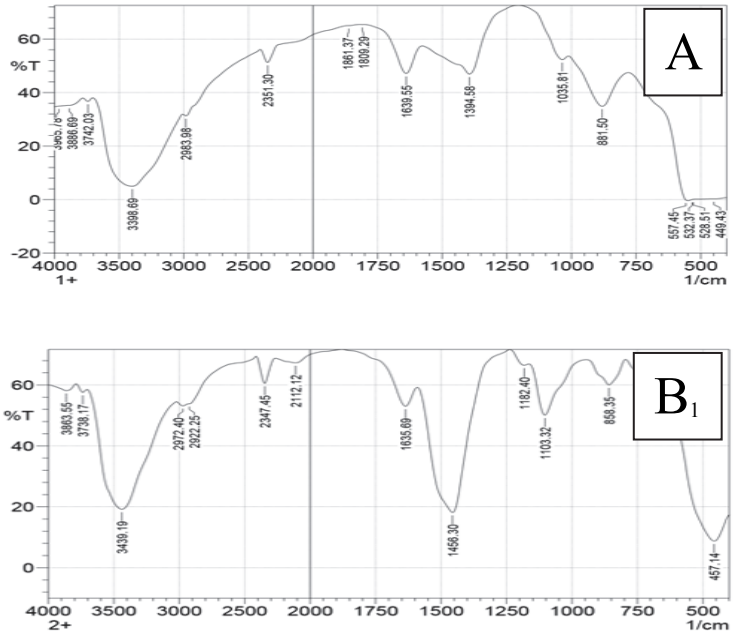

Figure 5. FTIR spectroscopy of chemical (A) and green (B_1) synthesis methods.

3.5 Thermal Properties of the Prepared Materials (TGA)

Figure 6 (A, B_1, and B_3) showed the thermal decomposition behavior of the chemical and green-synthesized ZnO nanoparticles over the studied temperature range of 0 to 600°C in N_2 atmosphere. With regard to chemical-synthesized zinc oxide nanoparticles, the first degradation step that started at 25°C and ended around 256°C is attributed to the evaporation of surface adsorbed water. The second and third thermal degradation step that start at 256°C and ended around 599°C may be caused by the decomposition of the condensation dehydration of the hydroxyls. The average sample weight loss for this temperature range for chemical-synthesized ZnO nanoparticles does not exceed 9.1% of the material weight, as shown in Figure 6 (A). The first degradation step of green-synthesized ZnO nanoparticles--that calcinated in an air heated furnace at 500°C for 2 hr before thermal decomposition and started at 19°C and ended around 200°C is attributed to the removal of surface waste adsorbed onto zinc oxide. The second thermal degradation that started at 200°C and ended around 598°C is attributed to the evaporation of surface adsorbed water and dehydration of the hydroxyls. The average sample weight loss for this temperature range for green-synthesized ZnO nanoparticles does not exceed 2.2% of the material weight. This result clearly indicates that the obtained powder has extreme purity as shown in Figure 6 (B_1). On the other hand, the first degradation step of green-synthesized ZnO nanoparticles paste that are non-calcinated before thermal decomposition and started at 38°C and ended around 93°C is attributed to the removal of surface waste adsorbed onto zinc oxide. The degradation that started at 93°C and ended around 177°C is attributed to the evaporation of surface adsorbed water, and then from 177°C to 282°C, the degradation may be caused by the decomposition of the condensation dehydration of the hydroxyls. The last thermal degradation step that started at 282°C and ended around 491°C might indicate the existence of organic material, in small amounts. The average sample weight loss for this temperature range for green-synthesized ZnO nanoparticles that does not exceed 51.6% of the material weight may be from the polyphenols or natural pigments that resulted from the plant leaf extract degradation shown in Figure 6 (B_3) [27, 28].

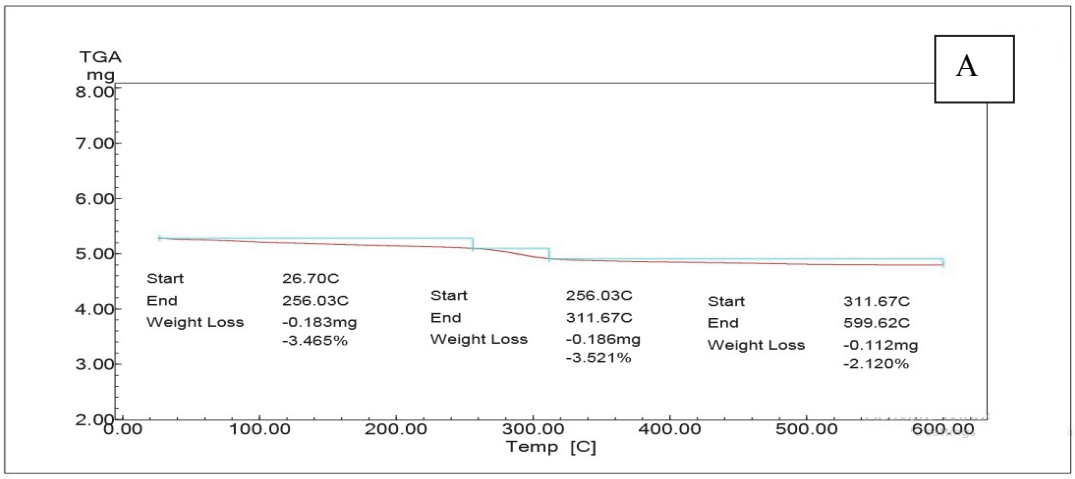

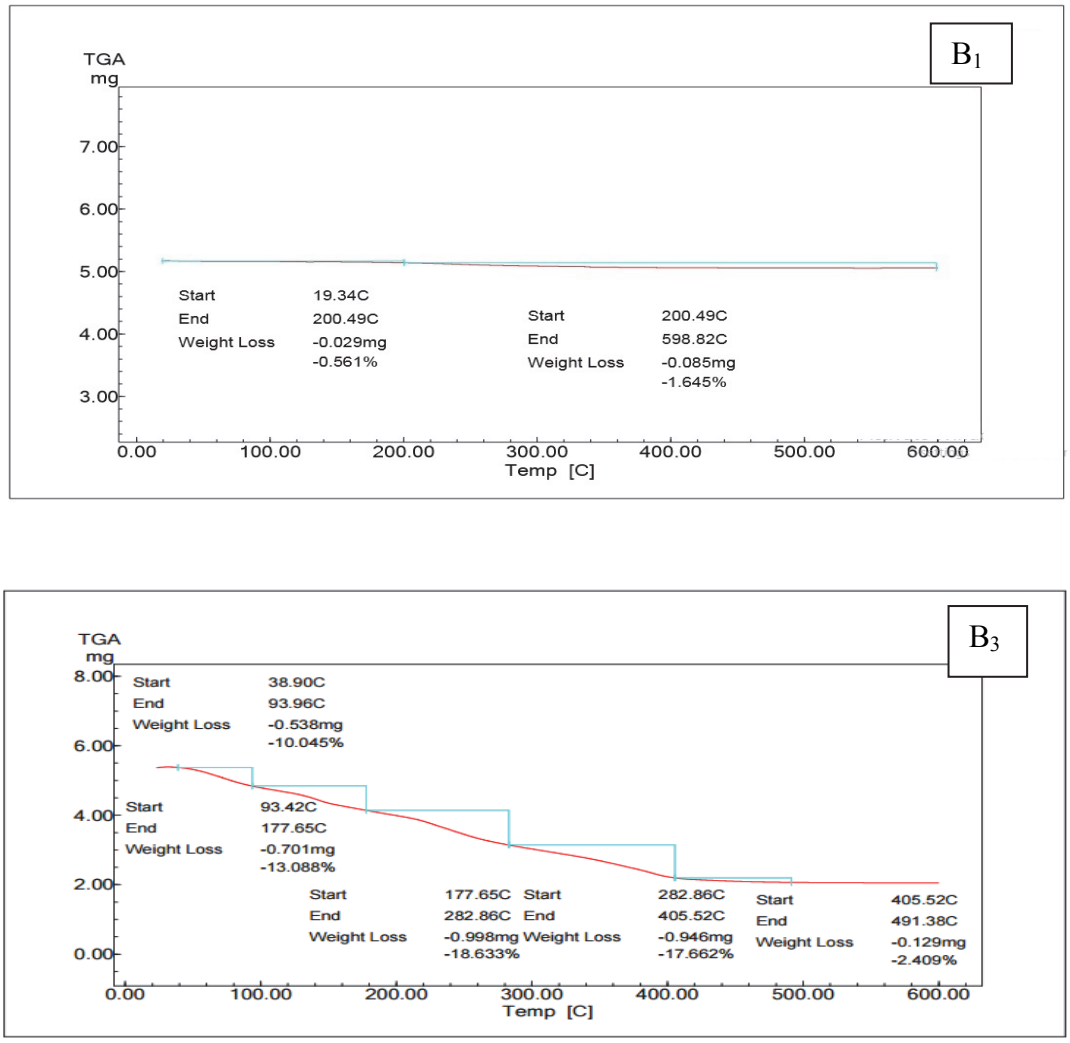

Figure 6. Thermo gravimetric analysis (TGA) for ZnO nanoparticles: (A) chemical, (B_1) green synthesis methods calcinated ZnO nanoparticles at 500˚C for 2 hr and (B_3) green synthesis methods without calcination of ZnO paste.

3.6 Particle Size Analysis (PSA)

A laser diffraction method with multiple scattering was used to determine the particle size distribution of the powder. The particle size distribution curve for ZnO nanoparticles synthesized using both chemical and green synthesis methods is shown in Figures 7 (A) and (B_1) respectively. The first peaks in Figures (7-A) and (8-B_1) that appear around 40 and 10nm represent chemical synthesized nanoparticles with a diameter of 9.2nm method and green-synthesized nanoparticles with a diameter of 8.2 nm respectively. The presence of the second peaks indicate that the average diameter is 526.6 nm for the chemical synthesis method and 197.6nm for the green synthesis method. The results correspond with the crystallite size calculated from the SEM and XRD patterns and it is also clear that the average diameter and particle size of the ZnO nanoparticles are smaller for the green synthesis method, compared with the chemical synthesis method.

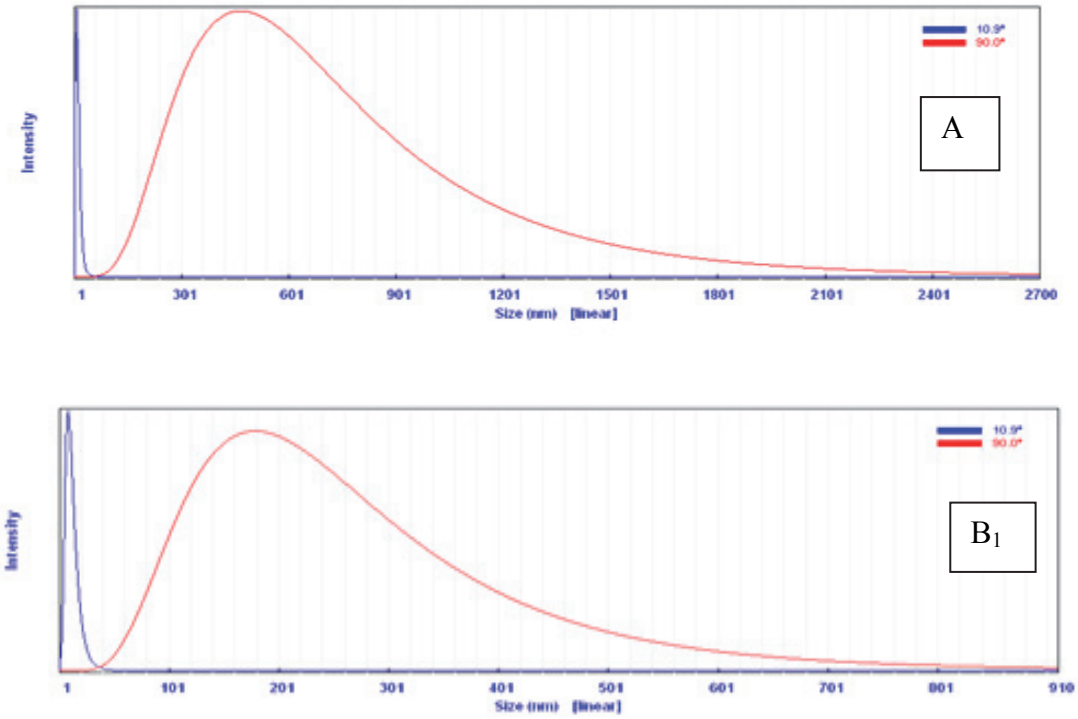

Figure 7. Particle Size Analysis (PSA) for ZnO nanoparticles (A) chemical and (B_1) green synthesis methods.

3.7 Assessment of the Green Synthetized Zno-Nps For Phenol Sorption

The kinetic adsorption profile of phenol onto ZnO-NPs indicated in Figure 8 was determined through the variation of contact time from 0 min to 250 min at the optimum concentration of phenol (5 ppm) with a dose of adsorbent (0.1gm), at pH 8, at a temperature of 25°C, and with agitation speed of 300 rpm. It is evident that phenol adsorption onto ZnO-NPs increases with increasing contact time. This result indicates that the large surface area of the prepared ZnO-NPs decreases the resistance against phenol diffusion, thus improving its mobility during the adsorption process with time [29]. Moreover, Figure 5 indicates that the contact time has a positive impact on the phenol adsorption onto ZnO-NPs. It is predicted from this behavior that the adsorption process is mainly diffusion-controlled. In conclusion, the adsorption affinity of phenol onto ZnO-NPs increases with increasing contact time until equilibrium state is reached [30].

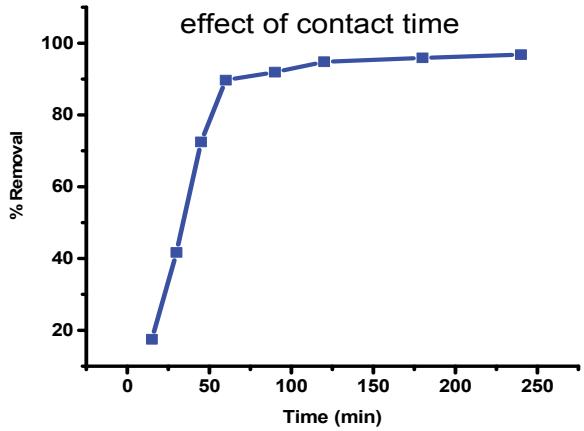

Figure 8. Effect of contact time on phenol removal onto green synthetized ZnO-NPs.

4. CONCLUSIONS

In the present study, it is found that biosynthesis as a green technology can be a good method for the synthesis of zinc oxide nanoparticles, when compared with chemical synthesis method. The bio-reduction of aqueous zinc ions using plant extracts of guava, olive, fig, and lemon plant leaves to produce ZnO nanoparticles has been demonstrated. The green chemistry technique characterized by various advantages such as simple to be scaled up, economically viable, easily available, familiar and eco-friendly. The obtained ZnO was characterized through XRD, SEM, TEM, FT-IR, TGA, and PSA analysis. It can be observed that the ZnO nanoparticles from both chemical and green synthesis methods have an almost-spherical shape with small agglomeration except when the green synthesis method is used with the olive extract, where the particles have an average particle size of 8-28nm, which corresponds with the crystallite size calculated from the SEM and XRD patterns. The thermal analysis results of the ZnO nanoparticles produced from chemical and green synthesis indicate that they possess thermal stability up to a temperature of 600°C. The green-synthetized ZnO-NPs were evaluated for phenol decontamination from polluted wastewater. It shows a maximum phenol removal of 99.7% within 150 minutes using 0.1g ZnO-NPs thus, making ZnO-NPs as promising adsorbent material for phenol decontamination from polluted wastewater.

REFERENCES

[1] M.F. Elkady, H. Shokry Hassan. Curr. Nanosci. **11** (2015) 805.
[2] E.T. Salem, R. A. Ismail, M.A. Fakhry, Y. Yusof, Int. J. Nanoelectronics and Materials **9** (2016) 111-122.
[3] M.F. Elkady, H. Shokry Hassan. Nanoscale Res. Lett. **10** (2015) 1.
[4] M. Shah, D. Fawcett, S. Sharma, S.K. Tripathy, G.E. Poinern, J. Materials. **8** (2015) 7278.
[5] M. F. Elkady, H. Shokry Hassan, E.E. Hafez, A. Fouad, Bioinorg. Chem. Appl. (2015) 20, Article ID 536854.
[6] C.N.R. Rao, S.R.C. Vivekchand, K. Biswasa, A. Govindaraj, J. Chem. Soc. Dalton Trans. **34** (2007) 3728.
[7] M. Akl Awwad, B. Albiss, A.L. Ahmad, J. Adv. Mat. Lett. **5** (2014) 520.
[8] O.J. Nava, P.A. Luque, C.M. Gómez-Gutiérrez, A.R. Vilchis-Nestor, A. Castro-Beltrán, M.L. MotaGonzález, A. Olivas, J. Mol. Struct. **12** (2016) 69.
[9] K. Elumalai, S. Velmurugan, J. Appl. Surf. Sci. **345** (2015) 329.
[10] Y.B. Saddeek, G.Y. Mohamed, H. Shokry Hassan, A.M.A. Mostafa, G. Abd elfadeel, J. Non-Cryst. Solids. **419** (2015) 110-117.
[11] J. El Ghoul, C. Barthou, L. El Mir, J. Superlattices Microstruct. **51** (2012) 942.
[12] D. Sarkar Tikku, S. Thapar, V. Srinivas, R.S. Khilar, J. Physicochem. Eng. **381** (2011) 123.
[13] G. Bandekar, N.S. Rajurkar, I.S. Mulla, U.P. Mulik, D.P. Amalnerkar, P.V. Adhyapak, J. Appl. Nanosci. **4** (2014) 199.
[14] E. R. Shaaban, M. El-Hagary, El Sayed Moustafa, H. Shokry Hassan, Yasser A. M. Ismail, M. Emam-Ismail, A. S. Ali, Appl. Phys. A **122** (2016) 1-10.
[15] B.W. Chieng, Y.Y. Loo, J. Mater. Lett. **73** (2012) 78.
[16] D. Ramimoghadam, M. Hussein and Y. Taufiq-Yap, J. Chem. Cent. **7** (2013)136.
[17] R.P.P. Singh, I.S. Hudiara, S. Panday, P. Kumar, S.B. Rana, Int. J. Nanoelectronics and Materials **9** (2016) 1-8.
[18] H. Shokry Hassan, M.F. Elkady, A.A. Farghali, Alaa Mohamed Salem, A.I. Abd El-Hamid, J. Taiwan Inst. Chem. Eng. **78** (2017) 307.
[19] A. Sathya, and V. Ambikapathy, J. Plant. Sci. Res. **4** (2012) 486.
[20] H. Michael Huang, S. Mao, H. Feick, H. Yan, Y. Wu, H. Kind, E. Weber, R. Russo, P. Yang, J. science. **292** (2001) 1897.
[21] D. Gnanasangeetha, D. SaralaThambavani, J. Res. Material Sci. **7** (2013) 1.

[22] Y.H. Tong, Y.C. Liu, S.X. Lu, L. Dong, S.J. Chen, Z.Y. Xiao, J. Sol-Gel .Sci .Tech. **30** (2004) 157.
[23] Z. Tao, X. Yu, J. Liu, L. Yang, S. Yang, J. Alloys Compd. **459** (2008) 395.
[24] R. zamari, A. Zakaria, H. Abbastar Ahangar, M. Darroudi, A. Zak and P.C. Gregor, J. Alloys Compd. **5** (2012) 41.
[25] J. Yang, X. liu, L. Yang, y. wang, Y. zhang, J. Lang, M. Gao, M. Wei, J. Alloys Compd. **46** (2009) 743.
[26] Q. Zhong, E. Matijevi´c, J. Mater. Chem. **6** (1996) 443.
[27] H. Shokry Hassan, M.F. Elkady, E.E. Hafez, E. Salama, Nanoscience and Nanotechnology-Asia. **7** (2017) 62.
[28] H. Shokry Hassan, M.F. Elkady, A. H. El-Shazly, H.S. Bamufleh. J. Nanomaterials. (2014) 14, Article ID 967492.
[29] E. R. Shaaban, M. El-Hagary, El Sayed Moustafa, H. Shokry Hassan, Yasser A. M. Ismail, M. Emam-Ismail, A. S. Ali, Appl. Phys. A **122** (2016) 1.
[30] M. El kady, H. Shokry, H. Hamad, RSC Advances **6** (2016), 82244.
[31] E.T. Salem, R. A. Ismail, M.A. Fakhry, Y. Yusof, Int. J. Nanoelectronics and Materials **9** (2016) 111-122.
[32] R.P.P. Singh, I.S. Hudiara, S. Panday, P. Kumar, S.B. Rana, Int. J. Nanoelectronics and Materials **9** (2016) 1-8.